

Non-ideal teleportation of tripartite entanglement: Einstein–Podolsky–Rosen versus Greenberger–Horne–Zeilinger schemes

Márcio M. Cunha¹ · E. A. Fonseca¹ · M. G. M. Moreno¹ · Fernando Parisio¹

Received: 29 November 2016 / Accepted: 20 August 2017 / Published online: 30 August 2017
© Springer Science+Business Media, LLC 2017

Abstract Channels composed by Einstein–Podolsky–Rosen (EPR) pairs are capable of teleporting arbitrary multipartite states. The question arises whether EPR channels are also optimal against imperfections. In particular, the teleportation of Greenberger–Horne–Zeilinger states (GHZ) requires three EPR states as the channel and full measurements in the Bell basis. We show that, by using two GHZ states as the channel, it is possible to transport any unknown three-qubit state of the form $c_0|000\rangle + c_1|111\rangle$. The teleportation is made through measurements in the GHZ basis, and, to obtain deterministic results, in most of the investigated scenarios, four out of the eight elements of the basis need to be unambiguously distinguished. Most importantly, we show that when both systematic errors and noise are considered, the fidelity of the teleportation protocol is higher when a GHZ channel is used in comparison with that of a channel composed by EPR pairs.

Keywords Teleportation · Entanglement · Noise

1 Introduction

Some findings have such a high degree of simplicity and relevance that become paradigms overnight. This is certainly the case of the quantum teleportation of an arbitrary, unknown qubit for the field of quantum information [1–3]. Of course, between

Electronic supplementary material The online version of this article (doi:10.1007/s11128-017-1705-9) contains supplementary material, which is available to authorized users.

✉ Fernando Parisio
parisio@df.ufpe.br

¹ Departamento de Física, Universidade Federal de Pernambuco, Recife, Pernambuco 50670-901, Brazil

the proof of possibility in principle [1] and an actual teleportation in the laboratory [2], there are several fundamental and practical difficulties. For example, in the original scheme, full measurements in a maximally entangled basis are required to obtain success in every run. This task, however, cannot be executed via linear one-qubit elements only, e. g., phase shifters and beam splitters [4,5]. Because of this, the first experimental implementation was conditional, requiring post-selection [2] (for unconditional implementations see, e. g., [6,7]). Even when complete measurements can be carried out, the channels and the measurement basis always present, to some extent, systematic (deviations from maximal entanglement) and random (environmental) imperfections.

A way to circumvent the difficulties related to the presence of noise is to resort to redundancy. In classical communications, it is usual to encode a single bit, say 0, as 000, so that error correction codes can recover the message with a prescribed success rate (note that an odd number of bits is required to avoid undecidable situations). Analogously, it is safer to encode the information contained in a single qubit $c_0|0\rangle + c_1|1\rangle$ in the larger state $c_0|000\rangle + c_1|111\rangle$ [8]. In fact, more than three qubits would be necessary to enable the correction of an arbitrary single-qubit error [8,9].

Another important use of Greenberger–Horne–Zeilinger (GHZ) states is as heralded Einstein–Podolsky–Rosen (EPR) pairs, since $|000\rangle + |111\rangle = |+\rangle|\Phi^+\rangle + |-\rangle|\Phi^-\rangle$, with $|\pm\rangle = (|0\rangle \pm |1\rangle)/\sqrt{2}$ and $|\Phi^\pm\rangle = (|00\rangle \pm |11\rangle)/\sqrt{2}$, so that a $+$ ($-$) detection in one of the parties heralds the existence of EPR entanglement $|\Phi^+\rangle$ ($|\Phi^-\rangle$) between the other two parties. In addition, several tasks in quantum computation demand more complex forms of entanglement, as for example, one-way quantum computing [10], for which graph states are needed.

It is, therefore, of evident interest to investigate efficient ways to teleport multiqubit entangled states. The most usual procedure is to employ as the channel a sufficient number of pairs of maximally entangled qubits, that is, EPR states. This is justifiable since bipartite entanglement is easier to prepare and serve as a universal resource for the teleportation of arbitrary states [11]. Particularly, the teleportation of three-particle states has been shown to be possible in several ways, being deterministic, for an ideal GHZ state via ideal EPR pairs [12], and, probabilistic for arbitrary three-particle states through a channel composed by non-maximally entangled EPR-like pairs [13]. The general problem of teleporting n -partite states with n EPR pairs has been addressed in [11,14] and carried out experimentally for the case of two qubits in [15].

There are, however, works where instead of EPR pairs, more complex states are used as quantum channels. One-qubit teleportation protocols are presented in [16] and [17], where GHZ states are employed, while in [18] a maximally entangled six-qubit state is used to teleport an arbitrary three-qubit state (see [19] for a scheme of controlled teleportation). In all these cases, the swapping operations that materialize the teleportation correspond to Bell measurements, that is, measurements in a bipartite entangled basis.

The question arises on what is the effect of systematically employing a channel of tripartite states and tripartite swapping operations in the teleportation of an unknown GHZ-like state. What are the final fidelities in comparison with a protocol that uses EPR pairs and measurements? In this work, we survey on the transport of GHZ-like states, $c_0|000\rangle + c_1|111\rangle$, with c_0 and c_1 unknown.

As a starting point, we develop a compact notation that encompass quite general protocols. We address the teleportation of three partite states through two different types of channels: (i) three EPR-type states and (ii) two GHZ-type states (in a particular geometric configuration). In addition, in scenario (i) the swapping is done using three Bell measurements, while in scenario (ii) two GHZ measurements are required. We refer to the first scheme as “3-EPR” and to the second one as “2 GHZ.” We show that in a totally ideal scenario (perfect channel and measurements without noise) the 3-EPR and 2-GHZ scheme lead to a fidelity of 100%, although the latter does not require complete GHZ measurements. We then proceed to investigate the individual and combined effects of systematic deviations from maximal entanglement, both in the channels and in the measurements, and of common types of noise.

Throughout this work, there will be nine qubits involved in each teleportation event. Six of these qubits (labeled 1 to 6) are close together, while the remaining three qubits (7, 8, and 9) are in a distant location. The GHZ-like state to be teleported is encoded in the odd-labeled qubits 1-3-5 and may be written as:

$$|\phi\rangle = \sum_{j=0,1} c_j |jjj\rangle. \tag{1}$$

Since this state is spatially localized and no part of it need to be physically moved in a preliminary stage, we will assume hereafter that it is protected from noise. For the other six qubits, forming the quantum channel, the entanglement is distributed among distant parties. In the final part of this work, we consider that the channels are not perfectly isolated from the environment, at least in some preparatory stage. In this weak noise regime, where the probability of an error occurring in one of the qubits is small, we find that the 2-GHZ scheme has a better performance. It is worth mentioning that, only recently a comprehensive account of the effects of practically relevant environmental disturbances was provided in the simplest case of the teleport of a qubit through an EPR channel [20].

2 Quantum teleportation

Let us briefly revisit the standard teleportation protocol to set our notation. It involves two distant parties, Alice and Bob, sharing a quantum channel consisting of a pair of entangled qubits in the state $\hat{\rho}_{ch}$. Alice intends to send an unknown quantum state $|\phi\rangle$ to Bob. She carries out a joint measurement in an orthonormal basis $\{|\Phi_K\rangle\}$ on her part of the channel and on the qubit to be sent. She classically informs Bob about her outcome. Finally, Bob applies a local unitary operation \hat{U}_K on his qubit. After each run, up to normalization, the state of Bob’s qubit is given by:

$$\hat{\rho}_K = \hat{U}_K \text{Tr}_A \left\{ \left(\hat{P}_K \otimes \hat{I}_B \right) |\phi\rangle \langle\phi| \otimes \hat{\rho}_{ch} \right\} \hat{U}_K^\dagger, \tag{2}$$

where \hat{P}_K is the projector $|\Phi_K\rangle \langle\Phi_K|$ and Tr_A denotes the partial trace over Alice’s system. Since, usually, the deviations from ideality are unknown, the unitary transformations \hat{U}_K refer to the ideal case of maximally entangled channels and measurements. The fidelity of the teleported state with respect to $|\phi\rangle$ reads

$$F = \sum_K \text{Tr} \{ |\phi\rangle \langle \phi| \hat{\rho}_K \}. \tag{3}$$

In general, F depends on the parameters that characterize the input state; thus, in order to get a state-independent figure of merit, we uniformly average over all possible input states:

$$\langle F \rangle = \frac{1}{V} \int dV F, \tag{4}$$

here, dV is the volume element on the space of quantum states and V is the total volume.

3 Fidelity of three-partite entanglement teleportation

In this section, we present details of the teleportation protocols and general fidelity expressions for both schemes proposed in this work: 3-EPR and 2-GHZ.

3.1 3-EPR scheme

We consider that each of the qubits 2, 4, and 6 is a half of an entangled pair, the other parties being qubits 7, 8, and 9, respectively, as summarized in Fig. 1. The density operator of each pair of the channel is represented by:

$$\hat{\rho}_{ab} = \sum_{klmn=0,1} \gamma_{klmn}^{(ab)} |kl\rangle \langle mn|, \tag{5}$$

where the coefficient $\gamma_{klmn}^{(ab)}$ already includes the information on deviations from ideality.

The measurement basis is not assumed to be ideal in the sense that its four kets may not be maximally entangled, although always orthonormal. In this case, we use the EPR-like basis $\{|\Psi_\lambda^\mu\rangle\}$ (see the supplementary material) to represent the measurements on pairs of qubits. Any element of this basis may be expressed as: $|\Psi_\lambda^\mu\rangle = \sum_{j=0,1} (-1)^{\mu j} b_{\mu \oplus j} |j, j \oplus \lambda\rangle$, where $b_0 = \cos \phi$, $b_1 = \sin \phi$, and \oplus stands for sum modulo 2. Note that for $\phi = \pi/4$, it corresponds to the Bell basis. Taking into account the three required measurements, the projector \hat{P}_K is

$$\hat{P}_K = |\Psi_\lambda^\mu\rangle \langle \Psi_\lambda^\mu|_{12} \otimes |\Psi_\omega^\nu\rangle \langle \Psi_\omega^\nu|_{34} \otimes |\Psi_\tau^\epsilon\rangle \langle \Psi_\tau^\epsilon|_{56}. \tag{6}$$

For each output, after the appropriate exchange of classical information, local unitary transformations on the qubits 7, 8, and 9 must be executed. The necessary transformations can be compactly expressed as:

$$\hat{U}_K = \sum_{klm=0,1} a_\mu^k a_\nu^l a_\epsilon^m |k, l, m\rangle \langle k \oplus \lambda, l \oplus \omega, m \oplus \tau|, \tag{7}$$

with the coefficients a_μ^k defined in such a way that: $a_{\mu_1 \mu_2 \dots \mu_m}^{j_1 j_2 \dots j_n} \equiv (-1)^{(j_1 + j_2 + \dots + j_n) (\mu_1 + \mu_2 + \dots + \mu_m)}$.

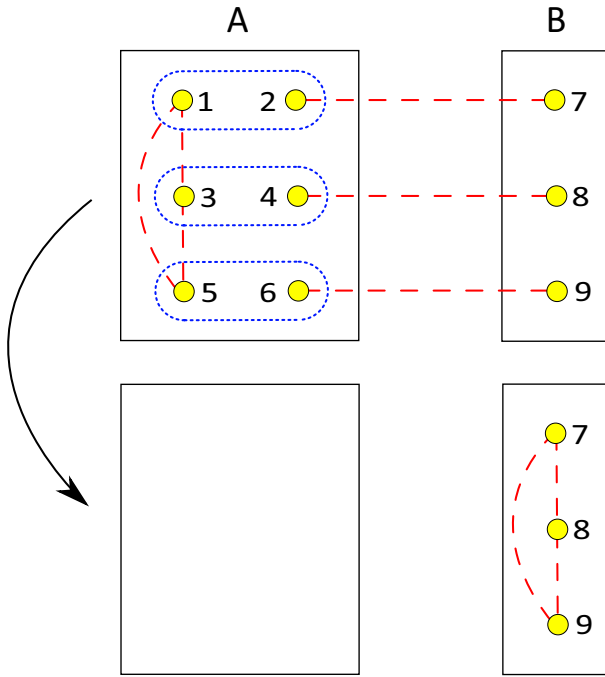


Fig. 1 Teleportation of an unknown state $\sum_{j=0,1} c_j |jjj\rangle_{135}$ through a channel composed by three EPR states. The *dotted ovals* represent complete measurements in the EPR basis $\{|\Psi_\lambda^\mu\rangle\}$ and the *dashed lines*, entanglement between the involved qubits

The local character of the unitaries is made explicit via the equivalent, separable expression

$$\hat{U}_K = \hat{\sigma}_z^\mu \hat{\sigma}_x^\lambda \otimes \hat{\sigma}_z^\nu \hat{\sigma}_x^\omega \otimes \hat{\sigma}_z^\epsilon \hat{\sigma}_x^\tau, \tag{8}$$

where the standard notation for the Pauli matrices has been employed. After some algebra, the fidelity reads:

$$F = \sum_{\substack{klmn\mu\nu \\ \epsilon\lambda\omega\tau=0,1}} c_k c_l^* c_n c_m^* a_{\mu\nu\epsilon}^{klmn} \prod_{j=1}^3 b_{\mu_j \oplus k}^* b_{\mu_j \oplus l} \gamma_{k \oplus \lambda_j, m \oplus \lambda_j, l \oplus \lambda_j, n \oplus \lambda_j}^{(a_j b_j)}, \tag{9}$$

where the index j is related to the channel qubits and measurements; thus, in order to get a compact expression, we wrote: $\{\lambda_1, \lambda_2, \lambda_3\} = \{\lambda, \omega, \tau\}$ and $\{\mu_1, \mu_2, \mu_3\} = \{\mu, \nu, \epsilon\}$.

This expression will be used later to calculate fidelity of the 3-EPR teleportation protocol for several specific cases.

3.2 2-GHZ scheme

In what follows we closely follow the previous procedure, this time, replacing the 3-EPR with the 2-GHZ scheme. The properties of this kind of tripartite state working

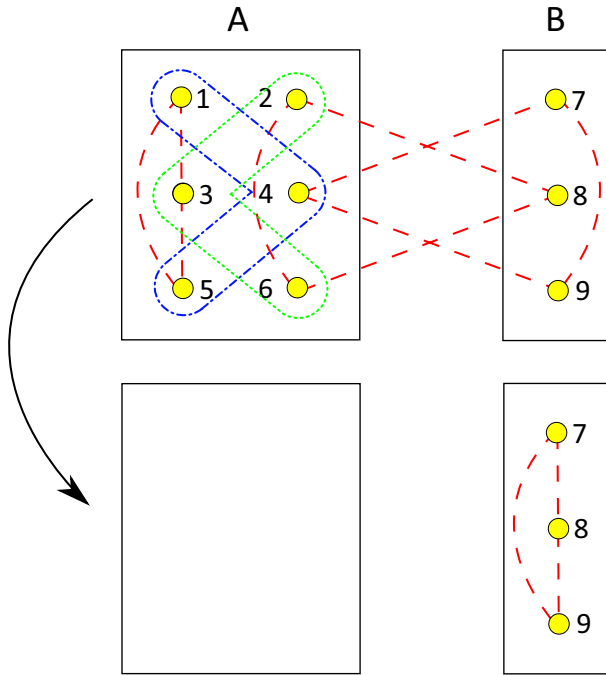


Fig. 2 Teleportation of an unknown state $\sum_{j=0,1} c_j |jjj\rangle_{135}$ through a channel composed by two GHZ states. Measurements in the GHZ-like basis $\{|\Psi_{\lambda\omega}^\mu\rangle\}$ are represented by *dotted* and *dot-dashed lines*, while entanglement between qubits by *dashed lines*

as a part of a channel have been investigated in different contexts. GHZ channels have been shown to be capable of transporting a single qubit [16, 17], and, in reference [21], e. g., it is shown that a bipartite entangled state, shared by two distant parties, *A* and *C* can be fully transported to other two distant parties, *B1* and *B2*, whenever *A*, *B1*, and *B2* share a GHZ state. Here, as in the previous section, we deal with the teleport of a GHZ-like state.

Of course, in order to make comparisons the input state, qubits 1–5, is exactly the same as before, Eq. (1). Furthermore, the channel corresponds to two tripartite states, which brings an important difference between the 3-EPR and 2-GHZ setups. In the first case qubits 2, 4, and 6 are completely equivalent, the same holding for qubits 7, 8, and 9. This is not possible in distributing these six qubits between two tripartite states. The only configuration that keeps the original distribution is the alternate geometry shown in Fig. 2. In this situation, qubits 2 and 6 are not equivalent to qubit 4, the same being valid for qubits 7 and 9 with respect to qubit 8. Analogously to the previous case, we express the density operator associated with the part of the channel involving the qubits *a*, *b*, and *c* as:

$$\hat{\rho}_{abc} = \sum_{\substack{klmn \\ pq=0,1}} \gamma_{klmnpq}^{(abc)} |klm\rangle \langle npq|. \tag{10}$$

In this case, we consider the non-maximally entangled GHZ-like measurement basis for $N = 3 \{|\Psi_{\lambda\omega}^\mu\rangle\}$, whose elements are given by (see the supplementary material): $|\Psi_{\lambda\omega}^\mu\rangle = \sum_{j=0,1} (-1)^{\mu j} b_{\mu\oplus j} |j, j \oplus \lambda, j \oplus \omega\rangle$, and the coefficient $b_{\mu\oplus j}$ defined in the same way as in the previous case. The projector related to the two necessary measurements reads:

$$\hat{P}_K = |\Psi_{\lambda\omega}^\mu\rangle \langle\Psi_{\lambda\omega}^\mu|_{145} \otimes |\Psi_{\tau\epsilon}^\nu\rangle \langle\Psi_{\tau\epsilon}^\nu|_{236}. \tag{11}$$

In principle, there would be $8 \times 8 = 64$ possible combinations of results (the same number as in the EPR case). However, there are four individual outputs that *never* occur. These zero-probability results are those with $\omega \neq 0$. Therefore, there are $4 \times 8 = 2^5 = 32$ possible results, corresponding to 5 bits of classical information and as we will show in the following sections, in several cases there is an additional constraint ($\epsilon = 0$) which reduces to 16 the number of possible outputs and 4 bits of classical communication. This means that full measurements in the GHZ-like basis are not necessary, as it happens in the 3-EPR scheme.

After some algebra, we find the local unitary transformations required on the qubits 7, 8, 9:

$$\hat{U}_K = \sum_{klm=0,1} a_\mu^k a_\nu^{l\oplus\tau} |k, l, m\rangle \langle k \oplus \lambda, l \oplus \tau, m \oplus \lambda|,$$

which is equivalent to:

$$\hat{U}_K = \hat{\sigma}_z^\mu \hat{\sigma}_x^\lambda \otimes \hat{\sigma}_x^\tau \hat{\sigma}_z^\nu \otimes \hat{\sigma}_x^\tau. \tag{12}$$

Thus, the fidelity of the teleportation protocol under the 2-GHZ scheme may be calculated. It reads:

$$F = \sum_{\substack{klmn\mu \\ v\tau\epsilon\lambda=0,1}} c_{k'} c_{l'}^* c_{n'} c_m^* a_{\mu\nu}^{klmn} b_{\mu\oplus k'}^* b_{\mu\oplus l'} b_{v\oplus l} b_{v\oplus k}^* \gamma_{k,k\oplus\epsilon,m,l,l\oplus\epsilon,n}^{(268)} \gamma_{k'\oplus\lambda,m'\oplus\lambda,m'\oplus\lambda,l'\oplus\lambda,n'\oplus\lambda,n'\oplus\lambda}^{(479)} \tag{13}$$

where the primed indexes j' stand for $j \oplus \tau$.

4 Non-maximally entangled channels and measurements

In this section, we assume that the systems in consideration are isolated and that any deviation from ideality comes from imperfections in measurements and in the preparation of the channel states.

4.1 3-EPR scheme

The channel of the 3-EPR scheme is composed by three pairs of qubits, which will be assumed to present some systematic deviation from maximal entanglement. We denote

the state of each pair composing the channel as $|\psi\rangle = \sum_{j=0,1} \beta_j |jj\rangle$, with $\beta_0 = \cos \theta$ and $\beta_1 = \sin \theta$, which, by inspection of Eq. (5), leads to $\gamma_{klmn}^{(ab)} = \beta_k \beta_m \delta_{kl} \delta_{mn}$. By replacing these ingredients in the general expression (9), we get:

$$F = |c_0|^4 + |c_1|^4 + 128|c_0|^2|c_1|^2 (b_0 b_1 \beta_0 \beta_1)^3. \tag{14}$$

In order to calculate the average fidelity, the input state can be parametrized as $(c_0, c_1) = (\cos \theta_0, e^{i\varphi} \sin \theta_0)$, with $0 < \theta_0 < \pi/2$ and $0 < \varphi < 2\pi$. The associated volume element is $dV = \sin \theta_0 \cos \theta_0 d\theta_0 d\varphi$, and the total volume is $V = \pi$. The average fidelity of the 3-EPR teleportation scheme under non-maximally entangled channels and measurements takes the form:

$$\langle F_{\text{EPR}} \rangle = \frac{2}{3} + \frac{1}{3} \sin^3(2\theta) \sin^3(2\phi). \tag{15}$$

If one assumes that the systematic errors are small, $\theta = \pi/4 + \delta\theta$ and $\phi = \pi/4 + \delta\phi$, then, since the first non-vanishing correction is quadratic in the deviations [$\langle F_{\text{EPR}} \rangle \approx 1 - 2(\delta\theta^2 + \delta\phi^2)$], the fidelity remains close to 1. As a numeric example, consider the deviations $\delta\theta = \delta\phi = 5^\circ$, which lead to $\langle F_{\text{EPR}} \rangle = 0.969$. We postpone the analysis of random (non-systematic) errors to the final part of this work where several common types of noise will be considered.

4.2 2-GHZ scheme

Following the same approach as in the previous case, the channel is composed of two initially prepared GHZ-like states $|\psi\rangle = \sum_{j=0,1} \beta_j |jjj\rangle$; thus, the γ coefficients become $\gamma_{klmnpq}^{(abc)} = \beta_k \beta_n \delta_{kl} \delta_{lm} \delta_{np} \delta_{pq}$. Substituting into the expression for the fidelity, Eq. (13) and after some calculations, we have:

$$F = |c_0|^4 + |c_1|^4 + 32|c_0|^2|c_1|^2 (b_0 b_1 \beta_0 \beta_1)^2. \tag{16}$$

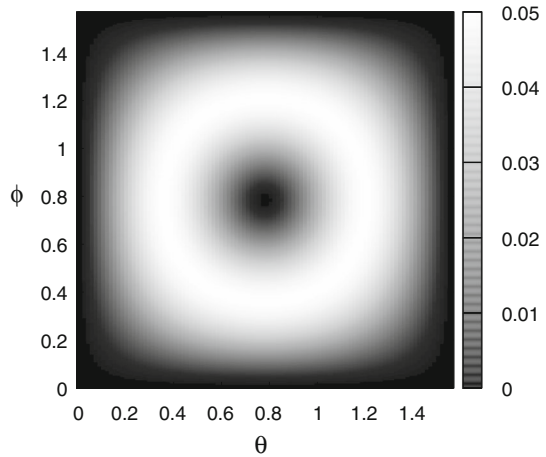
In addition, due to the configuration of the channel and measurements, the probability of the output corresponding to $\epsilon \neq 0$ is null, which reduces the number of possible outputs to 16.

In the same way as before, we calculated the average fidelity of the 2-GHZ teleportation scheme under non-maximally entangled channels and measurements. It reads:

$$\langle F_{\text{GHZ}} \rangle = \frac{2}{3} + \frac{1}{3} \sin^2(2\theta) \sin^2(2\phi), \tag{17}$$

which is larger than $\langle F_{\text{EPR}} \rangle$, for equal values of θ and ϕ . For small deviations from ideality, $\theta = \pi/4 + \delta\theta$ and $\phi = \pi/4 + \delta\phi$, we get $\langle F_{\text{GHZ}} \rangle \approx 1 - \frac{4}{3}(\delta\theta^2 + \delta\phi^2)$. Taking, as in the previous case, $\delta\theta = \delta\phi = 5^\circ$, we obtain $\langle F_{\text{GHZ}} \rangle = 0.979$, which presents a slight improvement with respect to the EPR channel.

Fig. 3 Difference of average fidelities, ΔF [Eq. (18)], produced by non-maximally entangled channels and measurements, as a function of θ and ϕ . The maximal difference $\Delta F = 4/81$ is attained for $\sin(2\theta) \sin(2\phi) = 2/3$



To have a more comprehensive picture, let us define the difference

$$\Delta F = \langle F_{\text{GHZ}} \rangle - \langle F_{\text{EPR}} \rangle, \tag{18}$$

which is nonnegative, showing that the GHZ channel has a better performance in comparison with the usual EPR channel (see Fig. 3). The difference attains its maximum value whenever channels and measurement bases satisfy $\sin(2\theta) \sin(2\phi) = 2/3$. In this situation, $\Delta F = 4/81 \approx 0.049$. In the next section, we will see that ΔF may reach even larger values if noise is present.

5 Weak noise regime

We now address the more realistic situation where, in addition to the systematic errors in the channels and in the swapping operations, random errors may appear. Here we will assume that the probabilities of occurrence of these errors in each of the six qubits composing a channel are statistically independent. We denote this probability by p . In addition, we will limit our analysis to situations where p is small enough so that one can safely disregard the possibility of more than a single error per channel. More precisely, the probability that no error occurs in a six-qubit channel is $\mathcal{P}_0 = (1 - p)^6$, while the chance that a single error occurs is $\mathcal{P}_1 = 6p(1 - p)^5$. We focus on the regime where this probability is much larger than that of two errors per set of six qubits, which is $\mathcal{P}_2 = 15p^2(1 - p)^4$, where we assumed that if the two errors happen in the same qubit, the overall effect is null (valid for bit flip and phase flip). Also we are not taking into account higher order events. Therefore a rough estimate for an upper bound for the usefulness of the next results is $p < p_{\text{max}} = 2/7 (\approx 0.29)$.

In the numeric example we provide in the end of this section, we consider a probability of error per qubit of 7% ($p = 0.07$) which leads to $\mathcal{P}_1 \approx 0.3$ and $\mathcal{P}_2 \approx 0.05$. In this scenario, there are only two typical occurrences. Either the channel is free from noise, or a random change happens to a single qubit. In what follows we address this

Table 1 Types of noise considered in the present work

Noise	Action	Kraus operators
Bit flip	$ 0\rangle \rightarrow 1\rangle, 1\rangle \rightarrow 0\rangle$	$\hat{A}_0 = \sqrt{1-p} \hat{1}, \hat{A}_1 = \sqrt{p} \hat{\sigma}_x$
Phase flip	$ 0\rangle \rightarrow 0\rangle, 1\rangle \rightarrow - 1\rangle$	$\hat{A}_0 = \sqrt{1-p} \hat{1}, \hat{A}_1 = \sqrt{p} \hat{\sigma}_z$
Bit-phase flip	$ 0\rangle \rightarrow i 1\rangle, 1\rangle \rightarrow -i 0\rangle$	$\hat{A}_0 = \sqrt{1-p} \hat{1}, \hat{A}_1 = \sqrt{p} \hat{\sigma}_y$
Depolarizing	Combined action of noises above	$\hat{A}_0 = \sqrt{1-p} \hat{1}, \hat{A}_j = \sqrt{\frac{p}{3}} \hat{\sigma}_j (j = x, y, z)$
Amplitude damping	Energy dissipation	$\hat{A}_0 = \begin{pmatrix} 1 & 0 \\ 0 & \sqrt{1-p} \end{pmatrix}, \hat{A}_1 = \begin{pmatrix} 0 & \sqrt{p} \\ 0 & 0 \end{pmatrix}$

problem by employing the Kraus-operator formalism to consider that the channels are not completely isolated from the environment. We will take into account the five common types of noise listed in Table 1.

The channels are initially prepared in non-maximally entangled states as in the previous section, and the action of noise through the Kraus operators on the state of the channels is introduced directly in the γ coefficients as we will show in each particular case.

5.1 Noisy EPR channel

We are in a position to turn our attention back to the 3-EPR channel subjected to random errors. In all cases, we start by considering that qubit 2 is the one affected by noise. Due to the equivalence between the three EPR states, the results must be the same for qubits 4 and 6 (see Fig. 1). For the EPR channel, it turns out that the effect of noise is also the same for the distant qubits 7, 8, and 9.

5.1.1 Bit flip

We start by considering a bit-flip error in qubit 2, the corresponding γ coefficient reads:

$$\gamma_{klmn}^{(27)} = \beta_l \beta_n \left\{ (1-p) \delta_{kl} \delta_{mn} + p \delta_{k,l \oplus 1} \delta_{m,n \oplus 1} \right\}. \tag{19}$$

It is then easy to obtain $\langle F \rangle_{(2)}$ as a function of $p, \theta,$ and ϕ and to show that the result remains unchanged when the error happens in any of the other five qubits of the channel. The final expression reads:

$$\langle F_{\text{EPR}}^{\text{B}} \rangle = (1-p) \left\{ \frac{2}{3} + \frac{1}{3} \sin^3(2\theta) \sin^3(2\phi) \right\}, \tag{20}$$

where ‘‘B’’ stands for bit flip. Therefore, the fidelity is globally affected by this type of noise.

5.1.2 Phase flip

Let us consider that the qubit 2 is probabilistically subjected to a phase flip, the γ coefficient is

$$\gamma_{klmn}^{(27)} = \beta_l \beta_n \delta_{kl} \delta_{mn} \left\{ 1 - p + p(-1)^{k \oplus m} \right\}. \tag{21}$$

Again, the result is the same for all six qubits of the channel, and the final result is

$$\langle F_{\text{EPR}}^{\text{P}} \rangle = \frac{2}{3} + \frac{1}{3}(1 - 2p) \sin^3(2\theta) \sin^3(2\phi). \tag{22}$$

Note that the classical part of this fidelity is not affected by the amount of noise, which is expected, since classical bits have no phase whatsoever.

5.1.3 Bit-phase flip

In this case, the γ coefficient is equal to:

$$\gamma_{klmn}^{(27)} = \beta_k \beta_m \left\{ (1 - p)\delta_{kl} \delta_{mn} + p(-1)^{k \oplus m} \delta_{k, l \oplus 1} \delta_{m, n \oplus 1} \right\}. \tag{23}$$

It leads to a fidelity:

$$\langle F_{\text{EPR}}^{\text{BP}} \rangle = (1 - p) \left\{ \frac{2}{3} + \frac{1}{3} \sin^3(2\theta) \sin^3(2\phi) \right\}, \tag{24}$$

which is equal to the fidelity of teleportation under bit flip noise.

5.1.4 Depolarizing

The γ coefficient under depolarizing noise is:

$$\gamma_{klmn}^{(27)} = \beta_l \beta_n \left\{ \left(1 - p + \frac{p}{3}(-1)^{k \oplus m} \right) \delta_{kl} \delta_{mn} + \frac{p}{3} \left(1 + (-1)^{k \oplus m} \right) \delta_{k, l \oplus 1} \delta_{m, n \oplus 1} \right\}. \tag{25}$$

The total fidelity amounts to:

$$\langle F_{\text{EPR}}^{\text{D}} \rangle = \frac{4}{9}p + \left(1 - \frac{4}{3}p \right) \left(\frac{2}{3} + \frac{1}{3} \sin^3(2\theta) \sin^3(2\phi) \right). \tag{26}$$

5.1.5 Amplitude damping

When amplitude damping noise affects the qubit 2, we have:

$$\gamma_{klmn}^{(27)} = \beta_l \beta_n \left\{ \alpha_l \alpha_n \delta_{k, l} \delta_{m, n} + p \delta_{l, k \oplus 1} \delta_{n, m \oplus 1} \delta_{l, 1} \delta_{n, 1} \right\}, \tag{27}$$

where $\alpha_0 = 1$ and $\alpha_1 = \sqrt{1 - p}$. The fidelity is:

$$\langle F_{\text{EPR}}^{\text{A}} \rangle = \frac{2}{3} \left(\cos^2 \theta + (1 - p) \sin^2 \theta \right) + \frac{\sqrt{1 - p}}{3} \sin^3(2\theta) \sin^3(2\phi). \tag{28}$$

In summary, the fidelity is globally compromised when either bit flip or bit-phase-flip noise is present, while only its quantum part is affected by phase flips, as expected. Depolarizing and amplitude damping noises present intermediate results. We recall that, in all situations, the particular channel qubit on which the error occurs is *immaterial*.

5.2 Noisy GHZ channel

Here we address the same types of noise, this time, acting upon a channel composed by two GHZ states. As we will see, the results may be quite different, both qualitatively and quantitatively. Here we initially consider that the qubit 6 may suffer random modifications. However, now, due to the distinct geometric distribution of entanglement, it is evident that qubit 6 and qubit 4, for instance, are inequivalent.

5.2.1 Bit flip

Consider the GHZ-like state of qubits 268 (see Fig. 2), with a possible flip in qubit 6. In this case, the channel coefficient reads:

$$\gamma_{klmnpq}^{(268)} = \beta_k \beta_n \delta_{km} \delta_{nq} \left\{ (1 - p) \delta_{kl} \delta_{np} + p \delta_{l, k \oplus 1} \delta_{p, n \oplus 1} \right\}. \tag{29}$$

After measurements, classical communication and unitary operations we get a quite remarkable result:

$$\langle F \rangle_{(6)} = \frac{2}{3} + \frac{1}{3} \sin^2(2\theta) \sin^2(2\phi), \tag{30}$$

which means that qubit 6 is fully protected from bit-flip noise. In contrast, when the same kind of noise is considered for the other five qubits, one obtains the ordinary result $\langle F \rangle_{(j)} = (1 - p) \langle F \rangle_{(6)}$, where $j = 2, 4, 7, 8, 9$. The final fidelity is given by $[\langle F \rangle_{(6)} + 5 \langle F \rangle_{(2)}] / 6$, that is:

$$\langle F_{\text{GHZ}}^{\text{B}} \rangle = \left(1 - \frac{5}{6} p \right) \left\{ \frac{2}{3} + \frac{1}{3} \sin^2(2\theta) \sin^2(2\phi) \right\}. \tag{31}$$

5.2.2 Phase flip

In the case of phase-flip noise, all six qubits in the channel become equivalent. Particularly, if qubit 2 is subject to phase-flip noise, we have:

$$\gamma_{klmnpq}^{(268)} = \beta_k \beta_n \delta_{kl} \delta_{lm} \delta_{np} \delta_{pq} \left\{ 1 - p + p(-1)^{l \oplus p} \right\}. \tag{32}$$

The final result is, in what concerns noise, analogous to that of the 3-EPR scheme:

$$\langle F_{\text{GHZ}}^P \rangle = \frac{2}{3} + \frac{1}{3}(1 - 2p) \sin^2(2\theta) \sin^2(2\phi). \tag{33}$$

The difference between $\langle F_{\text{GHZ}}^P \rangle$ and $\langle F_{\text{EPR}}^P \rangle$ comes exclusively from systematic errors.

5.2.3 Bit-phase flip

Since bit-phase flip is a combination of bit flip and phase-flip noises, the qubit 6 presents a different result from the other five, for this the channel coefficient reads:

$$\gamma_{klmnpq}^{(268)} = \beta_k \beta_m \delta_{km} \delta_{nq} \left\{ (1 - p) \delta_{kl} \delta_{np} + p(-1)^{l \oplus p} \delta_{l, k \oplus 1} \delta_{p, n \oplus 1} \right\}. \tag{34}$$

The corresponding fidelity is

$$\langle F \rangle_{(6)} = \frac{2}{3} + \frac{1}{3}(1 - 2p) \sin^2(2\theta) \sin^2(2\phi). \tag{35}$$

For the other five qubits, the fidelity holds:

$$\langle F \rangle_{(j)} = (1 - p) \left(\frac{2}{3} + \frac{1}{3} \sin^2(2\theta) \sin^2(2\phi) \right). \tag{36}$$

The final fidelity is:

$$\langle F_{\text{GHZ}}^{\text{BP}} \rangle = \left(\frac{2}{3} - \frac{10}{27} p \right) + \left(\frac{1}{3} - \frac{8}{27} p \right) \sin^2(2\theta) \sin^2(2\phi). \tag{37}$$

5.2.4 Depolarizing

As in the previous case, due to the Kraus operators that describe the depolarizing noise, the qubit 6 presents a different result from the other. The γ coefficient is:

$$\gamma_{klmnpq}^{(268)} = \beta_k \beta_n \delta_{km} \delta_{nq} \left\{ \left[1 - p + \frac{p}{3} (-1)^{l \oplus p} \right] \delta_{kl} \delta_{np} + \frac{p}{3} \left[1 + (-1)^{l \oplus p} \right] \delta_{l, k \oplus 1} \delta_{p, n \oplus 1} \right\}, \tag{38}$$

leading to a fidelity:

$$\langle F \rangle_{(6)} = \frac{2}{3} + \frac{1}{3} \left(1 - \frac{4}{3} p \right) \sin^2(2\theta) \sin^2(2\phi), \tag{39}$$

while, for the other five:

$$\langle F \rangle_{(j)} = \frac{2}{3} \left(1 - \frac{2}{3} p \right) + \frac{1}{3} \left(1 - \frac{4}{3} p \right) \sin^2(2\theta) \sin^2(2\phi), \tag{40}$$

The final expression for fidelity reads:

$$\langle F_{\text{GHZ}}^{\text{D}} \rangle = \frac{2}{3} \left(1 - \frac{5}{9}p \right) + \frac{1}{3} \left(1 - \frac{4}{3}p \right) \sin^2(2\theta) \sin^2(2\phi). \tag{41}$$

5.2.5 Amplitude damping

Finally, when amplitude damping noise affects qubit 6, the γ coefficient is:

$$\begin{aligned} \gamma_{klmnpq}^{(268)} = & \beta_k \beta_n \left(\alpha_k \alpha_n \delta_{kl} \delta_{lm} \delta_{np} \delta_{pq} \right. \\ & \left. + p \delta_{km} \delta_{nq} \delta_{k,1} \delta_{n,1} \delta_{l \oplus 1, k} \delta_{p \oplus 1, n} \right). \end{aligned} \tag{42}$$

The corresponding fidelity is

$$\langle F \rangle_{(6)} = \frac{2}{3} + \frac{\sqrt{1-p}}{3} \sin^2(2\theta) \sin^2(2\phi). \tag{43}$$

For the others qubits, we have:

$$\langle F \rangle_{(j)} = \frac{2}{3} \left\{ \cos^2 \theta + (1-p) \sin^2 \theta \right\} + \frac{\sqrt{1-p}}{3} \sin^2(2\theta) \sin^2(2\phi). \tag{44}$$

The total fidelity is

$$\langle F_{\text{GHZ}}^{\text{A}} \rangle = \frac{2}{3} \left(1 - \frac{5}{6}p \sin^2 \theta \right) + \frac{\sqrt{1-p}}{3} \sin^2(2\theta) \sin^2(2\phi). \tag{45}$$

5.3 Noisy GHZ channel using post-selection

In the scheme presented in the previous part, it is evident from the required unitary transformation (Eq. 12) that Alice needs to determine the values of μ, λ, ν and τ ($\omega = 0$ and ϵ is irrelevant), i.e., she only needs to discern among 4 out of the 8 elements of the GHZ basis in each measurement, and thus, 4 bits of classical communication are needed. However, we can improve the efficiency of the protocol if we note that in the presence of some classes of noise either on qubit 2 or 6, outputs corresponding to $\epsilon = 1$ come to appear and the state obtained in the Bob’s part of the system cannot be properly corrected by the unitary (Eq. 12). Then, in each step Alice may additionally inform Bob the value of ϵ , and he only uses the part of the ensemble corresponding to $\epsilon = 0$.

The general expression for the fidelity of teleportation is modified when post-selection is taken into account, after some calculations it becomes:

$$F = \frac{1}{1 - \sum_{\Gamma} p_m} \sum_{\substack{K \\ (K \notin \Gamma)}} \text{Tr} \{ |\phi\rangle \langle \phi| \hat{\rho}_K \}, \tag{46}$$

where Γ is the set of outcomes to be rejected and p_m is the probability of occurrence of the m -th output.

We calculated $p_{\epsilon=1}$ for all the kinds of noise considered in the present work on qubits 2 and 6; from this, we obtained expressions for average fidelity. Below we summarize the main results:

For bit-flip noise, we have $p_{\epsilon=1}^{(2)} = p_{\epsilon=1}^{(6)} = p$, and:

$$\langle F_{\text{GHZ}}^{\text{B-PS}} \rangle = \left(1 - \frac{2}{3}p \right) \left(\frac{2}{3} + \frac{1}{3} \sin^2(2\theta) \sin^2(2\phi) \right). \tag{47}$$

When bit-phase-flip noise is present, we get $p_{\epsilon=1}^{(2)} = p_{\epsilon=1}^{(6)} = p$, the fidelity holds:

$$\langle F_{\text{GHZ}}^{\text{BP-PS}} \rangle = \left(1 - \frac{2}{3}p \right) \left(\frac{2}{3} + \frac{1}{3} \sin^2(2\theta) \sin^2(2\phi) \right). \tag{48}$$

If depolarizing noise affects qubits 2 and 6, then $p_{\epsilon=1}^{(2)} = p_{\epsilon=1}^{(6)} = \frac{2p}{3}$, and:

$$\langle F_{\text{GHZ}}^{\text{D-PS}} \rangle = \frac{2}{3} - \frac{8}{27}p + \frac{1}{(9-6p)} \left\{ \left(3 - \frac{8}{3}p \right) u^2 - \frac{8}{3}p + \frac{16}{9}p^2u^2 \right\}, \tag{49}$$

where $u = \sin(2\theta) \sin(2\phi)$.

Finally, in the presence of amplitude damping noise, the probabilities show a dependence on the degree of entanglement of the channel, say: $p_{\epsilon=1}^{(2)} = p_{\epsilon=1}^{(6)} = p \sin^2 \theta$. In this case the average fidelity reads:

$$\langle F_{\text{GHZ}}^{\text{A-PS}} \rangle = \left(1 - \frac{2}{3}p \sin^2 \theta \right) \left\{ \frac{2}{3} + \frac{1}{3} \frac{\sqrt{1-p} \sin^2(2\theta) \sin^2(2\phi)}{1-p \sin^2 \theta} \right\}. \tag{50}$$

In the case of phase-flip noise on any qubit, the fidelity does not suffer modifications when compared with the scheme which makes no use of post-selection due to the fact that $p_{\epsilon=1}^{(2)} = p_{\epsilon=1}^{(6)} = 0$. Even with no null probabilities, a similar situation happens when bit-phase-flip noise is present, in this, no increase in the average fidelity is observed because of the combined action of both kinds of noise. For the other classes of errors, we found a remarkable improvement in the efficiency, as it can be seen in Table 2 for the specific case of maximally entangled channels and measurements.

6 Discussion and conclusion

Let us now summarize our results. In the absence of noise and with ideal (maximally entangled) channels and measurements, the two kinds of structures (3-EPR and 2-GHZ) lead to a fidelity of 100%. Still, while the 3-EPR scheme requires complete measurements in each run, the 2-GHZ scheme demands partial measurements.

As soon as systematic errors appear, in the form of non-maximally entangled channels and measurements, the fidelity obtained with the 2-GHZ setup is consistently

Table 2 Overall fidelity delivered by ideal 3-EPR, 2-GHZ and 2-GHZ-PS schemes, with ideal measurements and noise

Noise	3-EPR	2-GHZ	2-GHZ-PS
Bit flip	$1 - p$	$1 - \frac{5}{6}p$	$1 - \frac{2}{3}p$
Phase flip	$1 - \frac{2}{3}p$	$1 - \frac{2}{3}p$	$1 - \frac{2}{3}p$
Depolarizing	$1 - \frac{8}{9}p$	$1 - \frac{22}{27}p$	$\frac{2}{3} - \frac{8}{27}p + \frac{3 - \frac{16}{3}p + \frac{16}{9}p^2}{9 - 6p}$
Bit-phase flip	$1 - p$	$1 - \frac{2}{3}p$	$1 - \frac{2}{3}p$
A. damping	$\frac{2}{3} - \frac{1}{3}(p - \sqrt{1-p})$	$\frac{2}{3} - \frac{1}{3}(\frac{5}{6}p - \sqrt{1-p})$	$(1 - \frac{p}{3}) \left(\frac{2}{3} + \frac{1}{3} \frac{\sqrt{1-p}}{1 - \frac{p}{2}} \right)$

higher than that of the 3-EPR setup, see Eqs. (15–18) and Fig. 3. These results consider that all involved qubits are fully protected from environmental disturbances. Also, in this case no full measurements in the GHZ basis are required.

The opposite limiting situation is to consider ideal, maximally entangled measurements and channels ($\theta = \phi = \pi/4$), with noise afflicting the latter. These results are shown in Table 2 where, again, the 2-GHZ scheme presents better performances for bit-flip and depolarizing noises. Particularly remarkable is the fact that for any extent of bit-flip noise, due to the 2-GHZ structure of entanglement distribution and measurements, qubit 6 remains fully protected. For phase flips, the two structures lead to the same fidelity.

When all these imperfections are considered together, the 2-GHZ scheme is consistently more efficient than the 3-EPR one, as it can be seen by comparing the expressions for average fidelity in each particular case. The difference between the two schemes is more pronounced for non-ideal entanglement and bit-flip noise (see Fig. 4). In this case, it is easy to show that

$$\Delta F^B = \left\langle F_{\text{GHZ}}^{\text{B-PS}} \right\rangle - \left\langle F_{\text{EPR}}^{\text{B}} \right\rangle, \tag{51}$$

reaches its maximum for:

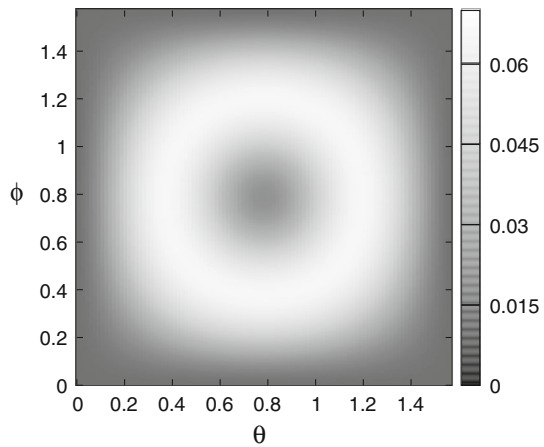
$$\sin(2\theta^*) \sin(2\phi^*) = \frac{2(1 - \frac{2}{3}p)}{3(1 - p)}. \tag{52}$$

For $p = 0.1$, we have $\Delta F^B \approx 0.07$.

The protocol is applicable to larger states of GHZ type, being scalable, in principle. In order to teleport a n-qubit GHZ state (GHZ_n), we may employ two GHZ_n states as the channel. It is possible to apply the measurement basis described in the Electronic Supplementary Material. For a GHZ with 4 particles, for example, a possible scheme is briefly described below. In this case, the initial state of the system is given by

$$\hat{\rho}_0 = \hat{\rho}_{1256} \otimes \hat{\rho}_{348(10)} \otimes \hat{\rho}_{48(11)(12)}. \tag{53}$$

Fig. 4 Plot of the difference of overall fidelities, ΔF^B [Eq. (51)], produced by 2-GHZ and 3-EPR channels, as a function of θ and ϕ for $p = 0.07$. Here, as in Fig. 3, *black* corresponds to $\Delta F^{bf} = 0$. The *lighter colors* present in this plot indicate that the difference between the two setups is more pronounced when noise is present



We can make measurements by using the basis $\{|\Phi_\lambda^\mu\rangle\}$:

$$|\Phi_\lambda^\mu\rangle = \sum_{j=0}^1 (-1)^{\mu j} b_{\mu \oplus \lambda} |j, j \oplus \lambda_1, j \oplus \lambda_2, j \oplus \lambda_3\rangle. \tag{54}$$

The measurements are made on the 1-2-3-4 and 5-6-7-8, after which the state in Bob’s side, up to normalization, is

$$\hat{\rho}_K = \text{Tr}_A \left\{ \left(\hat{P}_K \otimes \hat{I}_B \right) \hat{\rho}_0 \right\}, \tag{55}$$

where

$$\hat{P}_K = |\Psi_\lambda^\mu\rangle \langle \Psi_\lambda^\mu|_{1234} \otimes |\Psi_\tau^\nu\rangle \langle \Psi_\tau^\nu|_{5678}. \tag{56}$$

Analogously, it is possible to make a protocol with 5 particles and so on. Thus, it is possible to extend this idea to larger states.

Our general conclusion is that although EPR channels are extremely versatile in a wide variety of tasks, channels with more complex entanglement may be more resilient against systematic imperfections and noise in specific tasks.

Acknowledgements Financial support from Conselho Nacional de Desenvolvimento Científico e Tecnológico (CNPq) through its program INCT-IQ, Coordenação de Aperfeiçoamento de Pessoal de Nível Superior (CAPES), and Fundação de Amparo à Ciência e Tecnologia do Estado de Pernambuco (FACEPE) is acknowledged.

References

1. Bennet, C.H., et al.: Teleporting an unknown quantum state via dual classical and Einstein–Podolsky–Rosen channels. *Phys. Rev. Lett.* **70**, 1895–1899 (1993)
2. Bowmeester, D., et al.: Experimental quantum teleportation. *Nature* **390**, 575–579 (1997)
3. Pirandola, S., et al.: Advances in quantum teleportation. *Nat. Photonics* **9**, 641–652 (2015)

4. Mattle, K., et al.: Dense coding in experimental quantum communication. *Phys. Rev. Lett.* **76**, 4656 (1996)
5. Pan, J.-W., Zeilinger, A.: Greenberger–Horne–Zeilinger-state analyzer. *Phys. Rev. A* **57**, 2208 (1998)
6. Barrett, M.D., et al.: Deterministic quantum teleportation of atomic qubits. *Nature* **429**, 737–739 (2004)
7. Riebe, M., et al.: Deterministic quantum teleportation with atoms. *Nature* **429**, 734–737 (2004)
8. Barnett, S.M.: *Quantum Information*. Oxford University Press, Oxford (2008)
9. Steane, A.: Multiple-particle interference and quantum error correction. *Proc. R. Soc. Lond. A* **452**(1954), 2551–2577 (1996)
10. Raussendorf, R., Briegel, H.J.: A one-way quantum computer. *Phys. Rev. Lett.* **86**, 5188 (2001)
11. Cao, M., Zhu, S.-Q., Fang, J.-X.: Teleportation of n-particle state via n pairs of EPR channels. *Commun. Theor. Phys.* **41**, 689–692 (2004)
12. Yang, C.-P., Guo, G.-C.: A proposal of teleportation for three-particle entangled state. *Chin. Phys. Lett.* **16**, 628 (1999)
13. Fang, J., Lin, Y., Zhu, S., Chen, X.: Probabilistic teleportation of a three-particle state via three pairs of entangled particles. *Phys. Rev. A* **67**, 014305 (2003)
14. Ikram, M., Zhu, S.-Y., Zubairy, M.S.: Quantum teleportation of an entangled state. *Phys. Rev. A* **62**, 022307 (2000)
15. Zhang, Q., et al.: Experimental quantum teleportation of a two-qubit composite system. *Nat. Phys.* **2**(10), 678–682 (2006)
16. Almeida, N.G., et al.: One-cavity scheme for atomic-state teleportation through GHZ states. *Phys. Lett. A* **241**, 213–217 (1998)
17. Karlsson, A., Bourennane, M.: Quantum teleportation using three-particle entanglement. *Phys. Rev. A* **58**, 4394 (1998)
18. Long, Y., Qiu, D., Long, D.: Perfect teleportation between arbitrary split of six particles by a maximally genuinely entangled six-qubit state. *Int. J. Quantum Inform.* **08**, 821 (2010)
19. Nie, Y.-Y., et al.: Controlled teleportation of an arbitrary three-qubit state through a genuine six-qubit entangled state and Bell-state-measurements. *Int. J. Quantum Inform.* **09**, 763 (2011)
20. Fortes, R., Rigolin, G.: Fighting noise with noise in realistic quantum teleportation. *Phys. Rev. A* **92**, 012338 (2015)
21. Ghosh, S., Kar, G., Roy, A., Sarkar, D., Sen, U.: Entanglement teleportation through GHZ-class states. *New J. Phys* **4**(1), 48 (2002)